



# Green Synthesis of *Psidium guajava* Capped Hydroxyapatite Nanoparticles

P. Sindhuja\*, V. Kalaiselvi, N. Vidhya, V. Ramya

Department of Physics, Navarasam Arts and Science College for Women, Arachalur, Erode, TN, India

Received: 14.03.2020 Accepted: 28.04.2020 Published: 30-09-2020

\*sindhuja20598@gmail.com

## ABSTRACT

The current research focuses on the synthesis and characterization of hydroxyapatite nanoparticles of  $26 \pm 5$  nm size from *Psidium guajava* leaf extract with control over dimensions and composition. The reaction occurred very rapidly as the formation of spherical nanoparticles was almost completed within 30 min. The probable pathway of the green synthesis was suggested. Appearance, crystalline nature, size and shape of the nanoparticles were examined by Scanning Electron Microscopy, Energy Dispersive X-Ray Analysis, Fourier Transform Infrared Spectroscopy and X-Ray Diffraction techniques. A microwave-assisted route was selected for the synthesis of hydroxyapatite nanoparticles to carry out the reaction fast, suppress the enzymatic action and keep the process environmentally clean and green.

**Keywords:** Green synthesis; Hydroxyapatite nanoparticles; *Psidium guajava* leaf extract; Microwave.

## 1. INTRODUCTION

The process of removing toxic and waste metals in the environment including microorganisms, plants, and other biological structures can be achieved by means of oxidation, reduction or catalysis of metals with metallic nanoparticles. Metallic nanoparticles produced by biological methods are used in the biomedical field for purposes such as protection from harmful microorganisms, bio-imaging, drug transport, cancer treatment, medical diagnosis and sensor construction because of their unique properties such as insulating ability, antimicrobial and antioxidant nature, anti-metastasis, biocompatibility, stability and manipulability (Frasnelli *et al.* 2017).

Nanomaterials are the mainstay of nanotechnology that serve our lives for many years; they can be classified according to their origins, dimensions and structural configurations. Based on their origin, nanomaterials are classified into natural nanomaterials that are found in nature such as viruses, proteins, enzymes and minerals, and artificial nano-materials which are not found in nature and require some processes for their production (Gopi *et al.* 2014). The current research work was aimed at the synthesis of nanomaterials by green approach. Hydroxyapatite is synthesized with and without guava leaf extract and characterized.

## 2. MATERIALS & METHODS

### 2.1 Synthesis of Pure HAp Nanoparticles

The pure HAp nanoparticles were synthesized by taking 3.705 g of calcium hydroxide and 2.94 g of

orthophosphoric acid in separate beakers. Both the precursors were dissolved in the solvent - 50 ml of distilled water, under stirring of 30 min. After 30 minutes, orthophosphoric acid was mixed with calcium hydroxide solution under stirring and a gelatinous white precipitate was formed. Then, NaOH was added to maintain the pH at 12. The solution was aged for 24 hours at room temperature. Then the precipitate was washed and dried in a microwave oven at 75 W for 20 min. The dried sample was grained in mortar. The mixture was kept in a muffle furnace for 4 hours at  $400^\circ\text{C}$  to get a pure white fine powder.

### 2.2 Synthesis of capped HAp Nanoparticles

The same procedure was followed in capped Hydroxyapatite synthesis. *Psidium guajava* leaf extract was used as a solvent instead of distilled water.

## 3. CHARACTERIZATION TECHNIQUES

### 3.1 Fourier Transform Infrared Spectroscopy (FTIR)

FTIR is an analytical methodology used in industry and academic laboratories to understand the structure of individual molecules and the composition of molecular mixtures. FTIR spectroscopy uses modulated, mid-infrared energy to investigate a sample. The infrared light is absorbed in specific frequencies related to the vibrational bond energies of the functional groups present in the molecule. A characteristic pattern of bands is formed, which is the vibrational spectrum of the molecule (Kalaiselvi *et al.* 2017; 2019).

### 3.2 X-ray Powder Diffraction (XRD)

X-ray diffraction methods are the most effective techniques for determining the crystal structure of materials. X-ray diffractometry (XRD), was originally used for examining the crystal structure of powder samples; thus, traditionally, it is called X-ray powder diffractometry (Kalaiselvi *et al.* 2018a; 2018b). Wide-angle X-ray diffraction (WAXD) or wide-angle X-ray scattering (WAXS) is commonly used to characterize crystalline structures of polymers and fibers.

### 3.3 Scanning Electron Microscopy (SEM)

A typical SEM instrument has the electron column, sample chamber, EDS detector, electronics console and visual display monitors. The scanning electron microscope (SEM) uses a focused beam of high-energy electrons to generate a variety of signals at the surface of solid specimens. The signals that derive from electron-sample interactions reveal information about the sample, including external morphology (texture), chemical composition, crystalline structure and the orientation of materials making up the sample.

The SEM is also capable of performing analyses of selected point locations on the sample; this approach is especially useful in qualitatively or semi-quantitatively determining chemical compositions (using EDS), crystalline structure and crystal orientations (using EBSD). (Sundrarajan *et al.* 2015; Kumar *et al.* 2017). The design and function of SEM are very similar to Electron Probe Micro Analyzer (EPMA) and considerable overlap in capabilities exist between the two instruments.

### 3.4 Energy-Dispersive X-Ray Spectroscopy (EDAX)

Interaction of an electron beam with a sample target produces a variety of emissions, including X-rays. An energy-dispersive (EDAX) detector is used to separate the characteristic X-rays of different elements into an energy spectrum; EDAX system software is used to analyze the energy spectrum in order to determine the abundance of specific elements (Vasant *et al.* 2011; Yuan *et al.* 2017). EDAX can be used to find the chemical composition of materials down to a spot size of a few microns and to create element composition maps over a much broader raster area. Together, these capabilities provide fundamental compositional information for a wide variety of materials.

## 4. RESULTS & DISCUSSION

### 4.1 SEM

Fig.1. shows the SEM image of pure and capped HAp nanoparticles.

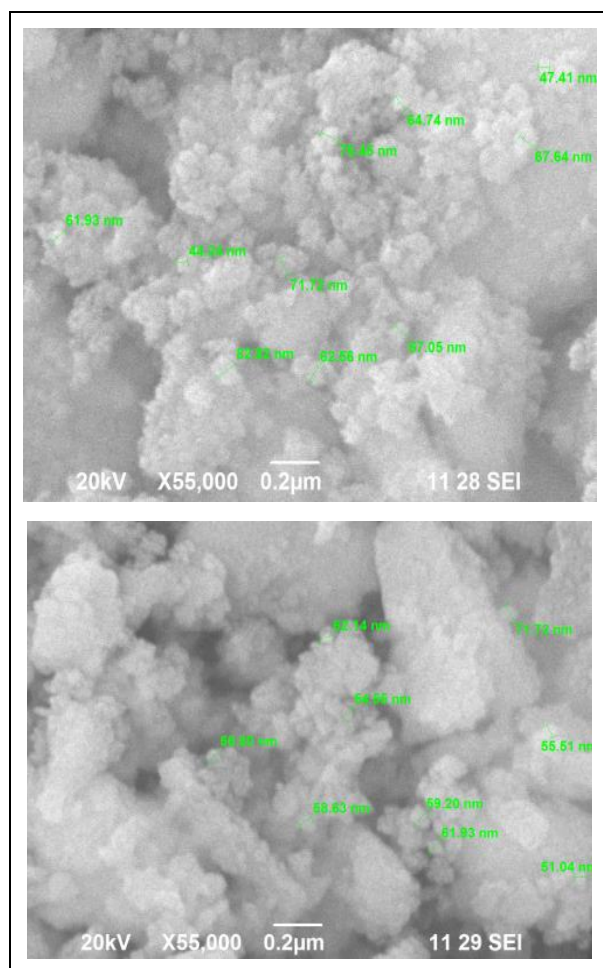


Fig. 1: SEM images of pure and capped HAp.

Table 1. XRD analysis HAP nanoparticles.

Element	App Conc	Intensity Corr.	Weight %	Weight % Sigma	Atomic %
O K	26.12	0.4387	51.23	0.61	70.08
Na K	2.35	0.6920	2.93	0.19	2.79
P K	19.90	1.3117	13.05	0.26	9.22
Ca K	38.39	1.0070	32.79	0.44	17.91
Total					100.00

### 4.2 Energy Dispersive X-Ray Diffraction Analysis

EDX results confirmed the obtained material, which is composed of Ca and P, as shown in Fig. 2 (a) and Ca, P and O, as shown in Fig. 2(b), for pure and capped HAp nanoparticles.

### 4.3 Fourier Transforms Infrared Spectroscopy

The FTIR spectra predicted the characteristic bands present in the sample. The presence of phosphate

and hydroxyl groups were identified, which corresponds to HAp structure. The FTIR spectrum of HAp has shown the vibration modes of phosphate at 870.70, 570.82 and 1044.26  $\text{cm}^{-1}$ . Hydroxyl groups of HAp were revealed at 3454.85 and 3744.12  $\text{cm}^{-1}$ . The vibration modes at 569.86, 872.631 and 1043.31  $\text{cm}^{-1}$  revealed the presence of phosphate and Hydroxyl groups at 3456.78  $\text{cm}^{-1}$  and 3636.12  $\text{cm}^{-1}$  for capped HAp.

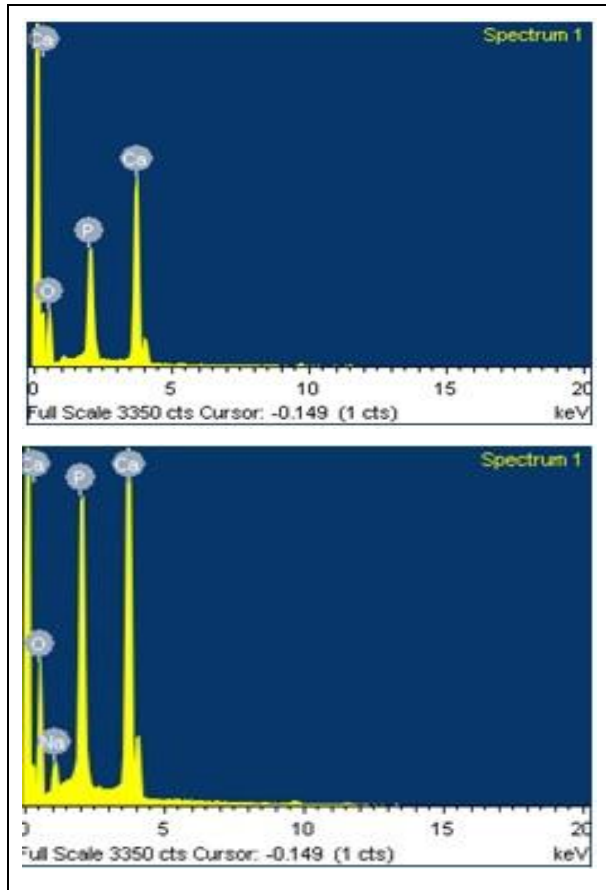


Fig. 2: EDAX images of pure and capped HAp.

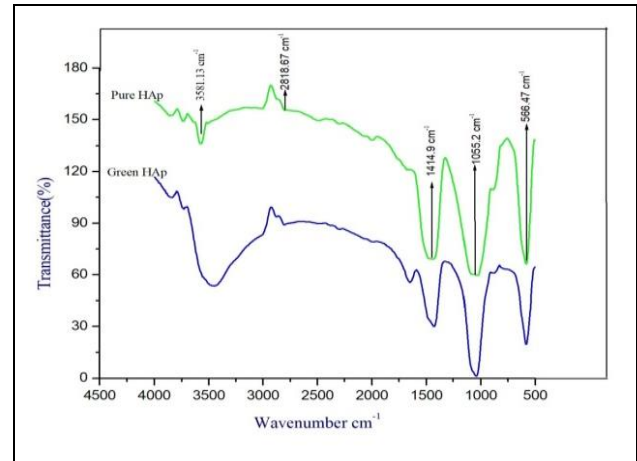


Fig. 3: FTIR images of pure and capped HAp.

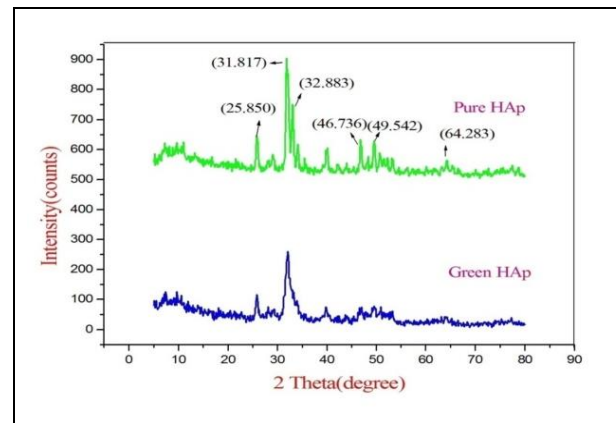


Fig. 4: XRD analyses of pure and Capped HAp nanoparticles.

#### 4.4 XRD Analysis

The XRD pattern of prepared pure HAp nanoparticles was shown in Fig. 4. The crystalline size of nanoparticles was determined from the major peak value. The average crystalline calculated by using Debye - Scherrer formula is approximately in the range between 5-24 nm.

Table 2. FTIR analyses of pure HAp and capped HAp nanoparticles.

S. No.	Sample	WAVE NUMBER $\text{cm}^{-1}$				
		O-H stretching vibration	stretching vibration	C=C stretching vibration	CH <sub>3</sub> stretching vibration	P-O Stretching vibration
1	P HAp	3555.67	2918.55	1593.81	1319.58	694.84
2	Capped HAp	3538.71	2916.49	1595.07	1317.41	695.18

Table 3. XRD analyses of pure HAp and capped HAp nanoparticles.

Sample	2θ (deg)	FWHM (deg)	D (Å)	Intensity (counts)	Crystalline size (nm)	Average crystalline size (nm)	hkl	Lattice constants		Unit volume
								a=b	C	
P HAp	31.97	0.7205	2.79	226	14.57	15.71	201	9.46	6.89	502.83
	35.97	0.3467	2.52	11	11.47		112			546.46
	39.10	0.4000	2.30	10	21.11		301			524.98
Capped HAp	32.13	1.32	2.78	128	6.23	8.54	112	9.48	6.84	531.07
	35.46	0.73	2.52	7	11.37		301			567.14
	39.82	1.05	2.26	21	8.04		212			500.64

## 5. CONCLUSION

The present study was carried out to synthesize Hydroxyapatite nanoparticles with and without capping agent *Psidium guajava* leaf extract irradiated by Microwave irradiation method. The XRD pattern confirmed the crystalline size of the sample; lattice parameter and unit cell volumes of nanoparticles were well-matched with the standard value. The crystalline size is lesser in capped HAp when compared with pure HAp. The FTIR spectrum revealed the presence of functional groups - phosphate and hydroxyl groups, in the sample. SEM analysis predicted the spherical-shaped morphological structure. Finally, EDAX analysis identified the elemental composition and purity of the sample, which was confirmed by the presence of calcium and phosphate groups.

## FUNDING

This research received no specific grant from any funding agency in the public, commercial, or not-for-profit sectors.

## CONFLICTS OF INTEREST

The authors declare that there is no conflict of interest.

## COPYRIGHT

This article is an open access article distributed under the terms and conditions of the Creative Commons Attribution (CC-BY) license (<http://creativecommons.org/licenses/by/4.0/>).



## REFERENCES

- Frasnelli, M., Cristofaro, F., Sglavo, V. M., Dirè, S., Callone, E., Ceccato, R., Bruni, G., Cornaglia, A. I., Visai, L., Synthesis and characterization of strontium-substituted hydroxyapatite nanoparticles for bone regeneration, *Mater. Sci. Eng., C* 71, 653–662 (2017).  
<https://dx.doi.org/10.1016/j.msec.2016.10.047>
- Gopi, D., Kanimozhi, K., Bhuvaneshwari, N., Indira, J., Kavitha, L., Novel banana peel pectin mediated green route for the synthesis of hydroxyapatite nanoparticles and their spectral characterization, *Spectrochim. Acta Part A Mol. Biomol., Spectrosc.*, 118, 589–597 (2014).  
<https://dx.doi.org/10.1016/j.saa.2013.09.034>
- Kalaiselvi, V., Mathammal, R., Synthesis and characterization of pure and triethanolamine capped hydroxyapatite nanoparticles and its antimicrobial and cytotoxic activities, *Asian J. Chem.*, 30(8), 1696–1700 (2018a).  
<https://dx.doi.org/10.14233/ajchem.2018.21214>
- Kalaiselvi, V., Mathammal, R., Vidhya, N., Surya, K., Synthesis and characterization of pure and capped hydroxyapatite nanoparticles, *Int. J. Adv. Sci. Eng.*, 6(1), 1213–1219 (2019).  
<https://dx.doi.org/10.29294/IJASE.6.1.2019.1213-1219>
- Kalaiselvi, V., Mathammal, R., Vijayakumar, S., Vaseeharan, B., Microwave assisted green synthesis of hydroxyapatite nanorods using *Moringa oleifera* flower extract and its antimicrobial applications, *Int. J. Vet. Sci. Med.*, 6(2), 286–295 (2018b).  
<https://dx.doi.org/10.1016/j.ijvsm.2018.08.003>

- Kalaiselvi, V., Mathammal, R., Anitha, P., Sol-Gel mediated synthesis of pure hydroxyapatite at different temperatures and silver substituted hydroxyapatite for biomedical applications, *J. Biotechnol. Biomater.*, <https://dx.doi.org/10.4172/2155-952X.1000275>
- Kumar, G. S., Rajendran, S., Karthi, S., Govindan, R., Girija, E. K., Karunakaran, G., Kuznetsov, D., Green synthesis and antibacterial activity of hydroxyapatite nanorods for orthopedic applications, *MRS Commun.*, 7(2), 183–188 (2017).  
<https://dx.doi.org/10.1557/mrc.2017.18>
- Sundrarajan, M., Jegatheeswaran, S., Selvam, S., Sanjeevi, N., Balaji, M., The ionic liquid assisted green synthesis of hydroxyapatite nanoplates by *Moringa oleifera* flower extract: A biomimetic approach, *Mater. Des.*, 88, 1183–1190 (2015).  
<https://dx.doi.org/10.1016/j.matdes.2015.09.051>
- Vasant, S. R., Joshi, M. J., Synthesis and characterization of pure and zinc doped calcium pyrophosphate dihydrate nanoparticles, *Eur. Phys. J. Appl. Phys.*, 53(1), 10601 (2011).  
<https://dx.doi.org/10.1051/epjap/2010100095>
- Yuan, Q., Wu, J., Qin, C., Xu, A., Zhang, Z., Lin, Y., Chen, Z., Lin, S., Yuan, Z., Ren, X., Zhang, P., One-pot synthesis and characterization of Zn-doped hydroxyapatite nanocomposites, *Mater. Chem. Phys.*, 199, 122–130 (2017).  
<https://doi.org/10.1016/J.MATCHEMPHYS.2017.06.047>